

characterized by a sudden increase in the $J=12$, $V=2$ and $J=10$ and 14 , $V=4$ components at the expense of the low- J , $V=0$ and 2 components. In this region, we have alignment between R and J so that $R=|I-J|$ dominates. J results from the parallel alignment of the spins of two valence particles. No further dramatic change occurs until the second backbend where the $J=16$, 18 , and 20 , $V=4$ components grow suddenly. Above this second backbend, these components continue to dominate the wave function. For $I=40$, the $J=20, R=20$ component enters with a probability of 76%. For $I=44$, the $J=20, R=24$ component has probability of 85%. Thus, the second backbend is characterized by the alignment of the spins of all four particles with R .

We believe that our simple model contains the necessary ingredients for a description of the rotation-alignment mechanism. We have four

particles in high-spin orbitals, a pairing interaction, and coupling to a strongly deformed, collective core. Our calculation of two backbends agrees qualitatively with the recent experimental observation in ^{158}Er . It seems likely, therefore, that the rotation-alignment mechanism can account for the ^{158}Er data. We have made no attempt to fit the experimental data by varying parameters. Details of this calculation will be published elsewhere.

¹I. Y. Lee *et al.*, Phys. Rev. Lett. **38**, 1454 (1977).

²R. A. Sorensen, Rev. Mod. Phys. **45**, 353 (1973); F. S. Stephens, Rev. Mod. Phys. **47**, 43 (1975).

³F. S. Stephens and R. S. Simon, Nucl. Phys. **A183**, 257 (1972).

⁴P. J. Evans and S. M. Harris, Nucl. Phys. **A277**, 109 (1977).

Isoscalar Breathing-Mode State in ^{144}Sm and ^{208}Pb

D. H. Youngblood, C. M. Rozsa, J. M. Moss, D. R. Brown, and J. D. Bronson
Cyclotron Institute and Physics Department, Texas A & M University, College Station, Texas 77843

(Received 7 September 1977)

Inelastic α -scattering experiments have been performed on ^{144}Sm and ^{208}Pb at $E_\alpha = 96$ MeV over the angular range $3^\circ \leq \theta_L \leq 8^\circ$. It is apparent that the isoscalar giant resonance in these nuclei consists of at least two broad components. The angular distribution for one component (^{144}Sm $E_x \sim 12.4$ MeV, ^{208}Pb $E_x \sim 11.0$ MeV) is well described as $E2$, while that for other component (^{144}Sm $E_x \sim 15.1$ MeV, ^{208}Pb $E_x \sim 13.7$ MeV) is well described by an $E0$ excitation exhausting approximately 100% of the $E0$ energy-weighted sum rule.

The location of the isoscalar breathing-mode state in nuclei has been the subject of considerable recent interest. The isoscalar giant resonance (GR) observed by inelastic scattering at an excitation energy of $\sim 63/A^{1/3}$ MeV in many nuclei was a possible candidate but has been considered to be predominantly quadrupole¹ (the GQR), exhausting a large fraction of the isoscalar $E2$ energy-weighted sum rule (EWSR).

From inelastic-electron-scattering experiments Pitthan *et al.*² have interpreted the 8.9-MeV state in ^{208}Pb as the breathing-mode state, but subsequent experiments³ have cast considerable doubt on that interpretation. Fukuda and Torizuka⁴ and Sasao and Torizuka⁴ have shown that their electron-scattering data on ^{90}Zr and ^{208}Pb are consistent with the existence of a breathing-mode state very near the isovector-dipole state (the giant-dipole resonance, GDR). This interpretation is critically dependent upon the model chosen for ex-

citation of the GDR, however. Marty *et al.*⁵ have suggested that differences in their inelastic deuteron data and our inelastic α spectra might be due to a breathing-mode state located just above the GQR in ^{40}Ca , ^{90}Zr , and ^{208}Pb .

In recent work by Harakeh *et al.*⁶ at Groningen utilizing inelastic α scattering at 120 MeV a shoulder on the higher excitation side of the GR has been identified in $^{206,208}\text{Pb}$, ^{197}Au , and ^{209}Bi . The angular distribution obtained from $12^\circ \leq \theta_L \leq 21^\circ$ for this shoulder is consistent with $L=0$, 2, or 4 transfer, although sum-rule arguments were advanced against an $L=2$ assignment.

In our earlier α -scattering studies¹ at 97 and 115 MeV and GR peak was observed to be asymmetric in many heavy nuclei. An analysis separating the GR peak into two components was performed for ^{141}Pr , ^{142}Nd , and $^{144,148,154}\text{Sm}$. The angular distributions for both components were the same within the uncertainties over the angular

range $13^\circ \leq \theta_L \leq 25^\circ$ hence the entire asymmetric peak was attributed to the GQR.

In this Letter we present new data which show that the inelastic α -scattering angular distributions for the two major components of the GR peak in ^{144}Sm and ^{208}Pb are substantially *different* for small angles ($3^\circ \leq \theta \leq 8^\circ$) and are consistent with the assignment of the higher excitation energy component (^{144}Sm $E_x = 15.1$ MeV, ^{208}Pb $E_x = 13.7$ MeV) as the isoscalar breathing-mode state exhausting $\sim 100\%$ of the $E0$ EWSR. The lower excitation component is the isoscalar quadrupole state which exhausts $\sim 90\%$ of the $E2$ EWSR.

Self-supporting metal-foil targets enriched to greater than 95% in the desired isotopes were bombarded with 96-MeV α particles from the Texas A & M University cyclotron. Inelastically scattered α particles were detected over an outgoing energy range of 50 MeV with an 86-cm-long resistive-wire proportional counter in the focal plane of an Enge split-pole magnetic spectrograph. The proportional counter was backed by a scintillator to provide both total energy and time signals. Signals from α particles were selected utilizing the energy and time-of-flight signals from the scintillator and the energy-loss signal obtained from the proportional counter. The signals were routed to a PDP-15 on-line computer and sums, divisions, and pulse selection were performed in real time.

Considerable care was taken to reduce effects of slit scattering and to insure the absence of spurious components in the beam. The solid-angle-defining slits at the entrance to the spectrograph were 1.5-mm-thick brass, polished to a mirror finish. The angular acceptance of the spectrograph for this experiment was limited to $\frac{1}{2}^\circ$ horizontally (to reduce angular averaging over the rapidly varying distribution) and $1\frac{1}{2}^\circ$ vertically (to remove the possibility of rays intercepting the pole faces and causing spurious spectral contributions). The beam was stopped on 5-mm-thick Ta attached to the defining slits and the beam current was integrated. Three x - y slit pairs were used after the exit slit of the 165° analyzing magnet as beam clean-up slits, but none were permitted to cut into the primary beam. A switching magnet affording a 10° bend between the first and second x - y slit pairs aided in cleaning out spurious beam. With the spectrograph at 2° and an empty target holder in place, the α spectrum was continuous in energy and the number of events obtained was negligible relative to the yield with the target in place. Spectra for ^{12}C , ^{48}Ti , and ^{208}Pb were taken

at $\theta_L = 2^\circ$, $2\frac{1}{2}^\circ$, and 3° (with the elastics blocked from the counter) to determine the effects of slit scattering. With the ^{12}C target the spectrum taken at 2° was clean and looked similar to those obtained at larger angles; with the ^{48}Ti target slit scattering was dominant at 2° but the GR was still quite visible, while at 3° the spectrum appeared much the same as at larger angles. With the ^{208}Pb target, slit scattering dominated the spectrum at 2° , but the GR was discernible at $2\frac{1}{2}^\circ$. The magnitude of the observed slit scattering is consistent with that found by Resmini *et al.*⁷ for polished-brass slits and followed roughly the Rutherford cross section as the target was changed. The beam-energy choice was a compromise; higher-energy beams enhance the giant-resonance yield relative to the continuum, but also move the first minimum in the angular distributions to smaller angles.

Data were taken on both ^{144}Sm and ^{208}Pb at 3° , $3\frac{1}{2}^\circ$, 4° , $4\frac{1}{2}^\circ$, 5° , 6° , 7° , and 8° with good statistics to ascertain the shape behavior of the GR peaks over these small angles. To reduce the chances of misinterpretation due to spurious contributions to the spectra, most of the data were taken a second time utilizing differing beam optics and spectrograph magnet settings. Additional data were taken on ^{144}Sm from 12° to 18° to allow normalization comparisons with data taken with counter telescopes. Relative normalizations were obtained from the integrated current for each run, while absolute normalizations were obtained from comparisons with counter data taken previously.¹

A ^{208}Pb spectrum taken at 4° and portions of the ^{144}Sm spectra taken at 3° , 4° , and 7° are shown in Fig. 1. The data were analyzed by fitting a multicomponent peak to the observed peak after subtraction of a nuclear continuum estimated with the procedure described in Ref. 1. For ^{208}Pb considerable fine structure was apparent on the GR peaks and fits consisting of four narrow Gaussian components plus two broad Gaussian components generally were necessary. For ^{144}Sm no fine structure was apparent so fits were restricted to two broad components. The data were best reproduced when the lower-excitation component was assumed to be somewhat asymmetric. The peak positions and widths obtained for the two broad components were consistent over the angular range studied and the values obtained are summarized in Table I. They are in excellent agreement with those obtained for ^{144}Sm by a similar analysis of our previous¹ counter data and for

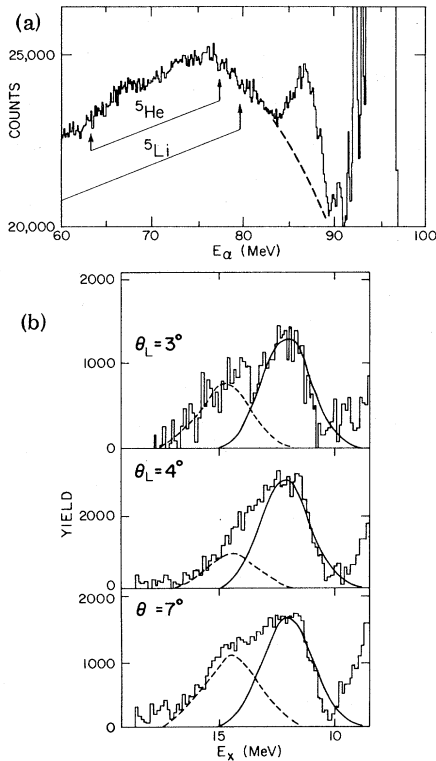


FIG. 1. (a) A $^{208}\text{Pb}(\alpha, \alpha')$ spectrum taken at $\theta_L = 4^\circ$. The dashed line indicates the background chosen. (b) A portion of $^{144}\text{Sm}(\alpha, \alpha')$ spectra ($E_\alpha = 96$ MeV) taken at 3° , 4° , and 7° are shown after subtraction of the continuum background. Gaussian peaks are shown for both components utilizing positions and widths from Table I.

^{208}Pb by Harakeh *et al.*⁶ The angular distribution obtained for the two broad components for both ^{144}Sm and ^{208}Pb are shown in Fig. 2. In each case the angular distributions for the two GR components are different as is apparent from the spectra shown in Fig. 1.

Distorted-wave Born-approximation (DWBA) calculations were performed using the computer code DWUCK.⁸ The calculations used were performed with the parameters listed in Ref. 1

TABLE I. Parameters obtained for the two components of the GR peak.

| | E_x (MeV) | Γ (MeV) | J^π | $\beta^2 R^2$ | EWSR (%) |
|-------------------|----------------|-------------------|---------|---------------|--------------|
| ^{144}Sm | 12.4 ± 0.4 | 2.6 ± 0.4 | 2^+ | 0.43 | 85 ± 15 |
| | 15.1 ± 0.5 | 2.9 ± 0.5 | 0^+ | 0.22 | 100 ± 20 |
| ^{208}Pb | 11.0 ± 0.2 | 2.7 ± 0.3 | 2^+ | 0.35 | 90 ± 20 |
| | 13.7 ± 0.4 | 3.0 ± 0.5 | 0^+ | 0.17 | 105 ± 20 |

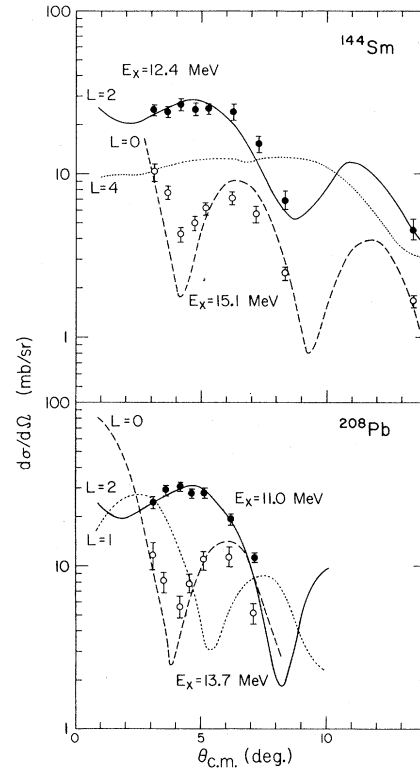


FIG. 2. Angular distributions obtained for both components of the giant resonance peaks in ^{144}Sm and ^{208}Pb . DWBA calculations are shown for several L transfers. The normalizations for the $L=1$ and $L=4$ calculations are arbitrary.

(^{148}Sm parameters were used for ^{144}Sm). Several optical-potential-parameter sets from the literature were tried, but the results were roughly independent of optical parameters. Monopole calculations were performed using both Satchler's⁹ version-1 and -2 form factors. The other form factors and sum rules used are discussed in Ref. 1. The magnitudes of the DWBA predictions changed somewhat with differing optical potentials, differing form factors (for the monopole), and differing Coulomb-excitation parameters; however, the shapes of the angular distributions were essentially unchanged. The predictions for a monopole state, the isovector-dipole state, a quadrupole state, and a hexadecapole state are shown superimposed on the data in Fig. 2. It is readily seen that the lower-excitation component is relatively well fitted by the quadrupole calculation, while the higher-excitation component is fitted adequately by the monopole calculation. In particular, the predicted signature of a monopole state, a sharp minimum around 4° , is very appar-

ent in the data for the higher-excitation component for both nuclei, while no such dip exists in the data for the lower-excitation component. The prediction for the GDR is out of phase with the data. The sum-rule fractions obtained are summarized in Table I; the uncertainties indicated reflect only an estimate of the uncertainty in normalization of the DWBA calculations to the data. Realistic uncertainties due to background choice and peak-fitting ambiguities are $\pm 50\%$ in the EWSR for the monopole state and 25% for the quadrupole state.

These results are in agreement with those of Refs. 4 and 5 for the location of the breathing-mode state in ^{208}Pb . The EWSR fraction obtained agrees with the value obtained at Sendai using a Gamow-Teller analysis and with the Harakeh *et al.*⁶ $L=0$ analysis. The $E0$ assignment suggests that the upper component observed¹ in ^{141}Pr , ^{142}Nd , and ^{148}Sm and in⁶ ^{206}Pb , ^{197}Au , and ^{209}Bi may also be predominantly monopole.

An energy of 13.7 MeV for the breathing mode in ^{208}Pb is in excellent agreement with several recent theoretical estimates.^{10,11} Utilizing the liquid-drop model, the breathing-mode energy is related to the nuclear-matter compressibility K by

$$E_0 = \frac{\pi}{3R} \left(\frac{\hbar^2 K}{m} \right)^{1/2},$$

where R is the nuclear radius and m is the nucleon mass. The use of $E_0 = 13.7$ MeV for ^{208}Pb and $E_0 = 15.1$ MeV for ^{144}Sm results in values for K of 208 and 197 MeV, respectively, in fair agreement with those predicted by Pandharipande.¹²

These values are typical of those obtained using realistic nuclear forces ($K \sim 150\text{--}200$ MeV) and are sharply lower than the values obtain with density-dependent Skyrme-type forces ($K \sim 300$ MeV).

This work was supported in part by the National Science Foundation and the Robert A. Welch Foundation.

¹D. H. Youngblood, J. M. Moss, C. M. Rozsa, J. D. Bronson, A. D. Bacher, and D. R. Brown, *Phys. Rev. C* **13**, 994 (1976).

²R. Pitthan, F. R. Buskirk, E. B. Dally, J. N. Dyer, and X. K. Maruyama, *Phys. Rev. Lett.* **33**, 849 (1974).

³A. Schwierczinski, R. Frey, A. Richter, E. Spamer, H. Theissen, O. Titze, Th. Walcher, S. Krewald, and R. Rosenfelder, *Phys. Rev. Lett.* **35**, 1244 (1975).

⁴S. Fukuda and Y. Torizuka, *Phys. Lett.* **62B**, 146 (1976); M. Sasao and Y. Torizuka, *Phys. Rev. C* **15**, 217 (1977).

⁵N. Marty, M. Morlet, A. Willis, V. Comparat, and R. Frascaria, in *Proceedings of the International Symposium on Highly Excited States in Nuclei, Jülich, Federal Republic of Germany, 1975*, edited by A. Faessler, C. Mayer-Boericki, and P. Turek (Kernforschungsanlage Jülich GmbH, Jülich, F.R.G., 1975), Vol. I, p. 17.

⁶M. N. Harakeh, K. van der Borg, T. Ishimatsu, H. P. Morsch, A. van der Woude, and F. E. Bertrand, *Phys. Rev. Lett.* **38**, 676 (1977).

⁷F. G. Resmini, A. D. Bacher, D. J. Clark, E. A. McClatchie, and R. De Swiniarski, *Nucl. Instrum. Methods* **74**, 261 (1969).

⁸Received from P. D. Kunz.

⁹G. R. Satchler, *Part. Nucl.* **5**, 105 (1973).

¹⁰S. Krewald, R. Rosenfelder, J. E. Galonska, and A. Faessler, *Nucl. Phys.* **A269**, 112 (1976).

¹¹J. Speth, L. Zamick, and P. Ring, *Nucl. Phys.* **A232**, 1 (1974).

¹²V. R. Pandharipande, *Phys. Lett.* **31B**, 635 (1970).